DESY 98-009
TTP 98-03
HD-THEP–98–3
hep-ph/9801419
January 1998

QCD Potential and $t\bar{t}$ Threshold Cross Section – Status Report –

M. Jeżabek[a)], J. H. Kühn[b)], M. Peter[c)], Y. Sumino[b)*] and T. Teubner[d)]

a) Institute of Nuclear Physics, Kawiory 26a, PL-30055 Cracow, Poland

b) Institut für Theoretische Teilchenphysik, Universität Karlsruhe, D-76128 Karlsruhe, Germany

c) Institut für Theoretische Physik, Universität Heidelberg, Philosophenweg 16, D-69120 Heidelberg, Germany

d) Deutsches Elektronen-Synchrotron (DESY), Notkestraße 85, D-22607 Hamburg, Germany

Abstract

We include the full second-order corrections to the static QCD potential in the analysis of the $t\bar{t}$ threshold cross section. Then we examine the difference between the results obtained in the momentum-space approach and in the coordinate-space approach, which was found recently. Contrary to our expectation, the reduction of the difference by the inclusion of the second-order corrections is very small. There still remains a non-negligible deviation, which originates from the difference in the construction of the potentials in the two spaces. We scrutinize this problem. In particular, we estimate our present theoretical uncertainty of the $t\bar{t}$ threshold cross section at the peak to be $\delta\sigma_{\rm peak}/\sigma_{\rm peak} \gtrsim 6\%$ within perturbative QCD.

*On leave of absence from Department of Physics, Tohoku University, Sendai 980-77, Japan.

In this paper we report on our present theoretical understanding of the $t\bar{t}$ total cross section near the threshold. Up to now, all the $\mathcal{O}(\alpha_s)$ corrections (also leading logarithms) have been included in the calculations of various cross sections near threshold. In order to take into account the QCD binding effects properly in the cross sections, we have to systematically rearrange the perturbative expansion near threshold. Namely, we first resum all the leading Coulomb singularities $\sim (\alpha_s/\beta)^n$, take the result as the leading order contribution, and then calculate higher order corrections, which are essentially resummations of the terms $\sim \alpha_s^{n+1}/\beta^n$, $\alpha_s^{n+2}/\beta^n, \ldots$ It is also important to resum large logarithms arising from the large scale difference involved in the calculation [1].* This is achieved by (first) calculating the Green function of the non-relativistic Schrödinger equation with the QCD potential [2, 1]. Conventionally both the coordinate-space approach developed in Refs. [1, 3] and the momentum-space approach developed in Refs. [4, 5] have been used in solving the equation by different groups independently. It has recently been found [6] that there are discrepancies in the results obtained from the two approaches reflecting the difference in the construction of the potentials in both spaces. It was argued that the differences are formally of $\mathcal{O}(\alpha_s^2)$ but their size turns out to be non-negligible.

Quite recently there has been considerable progress in the theoretical calculations of the second-order corrections to the cross section at threshold and the Coulombic bound-state problem. New contributions have been calculated analytically [7, 8] and numerically [9] for QED bound-states. Very important steps have been accomplished in QCD as well. The full second-order correction to the static QCD potential was computed in [10]. Also, the $\mathcal{O}(\alpha_s^2)$ total cross section is known now in the region $\alpha_s \ll \beta \ll 1$ as a series expansion in β [11]. All these results have to be included in the calculation of the full $\mathcal{O}(\alpha_s^2)$ corrections to the threshold cross section, which has been completed just in these days (as far as the production process of top quarks are concerned) [12].

In this report, we incorporate the full $\mathcal{O}(\alpha_s^3)$ corrections (the second-order corrections to the leading contribution) to the static QCD potential into our analyses. In principle this is a step towards an improvement of the theoretical precision in our analysis of the $t\bar{t}$ threshold cross section. The reduction of the difference is very small, however, and there still remains a non-negligible difference. We scrutinize this problem of the difference between the momentum-space and the coordinate-space potentials. We find that there is a theoretical uncertainty within perturbative QCD which limits our present-day theoretical accuracy of the threshold cross section.

Let us first state the numerical accuracies attained throughout our analyses. We confirmed that our numerical accuracies are at the level of 10^{-4}. We have tested our programs with the Coulomb potential whose analytical form is known both in momentum space and in coordinate space. Moreover we confirmed that we obtain the same cross section within the above accuracy, irrespective of whether we solve the Schrödinger equation in momentum space or first Fourier transform the potential and solve the Schrödinger equation in coordinate space. In this way we also checked that our numerical Fourier transformation of the potential (from momentum space to coordinate space) works within the above quoted accuracy. The level of accuracies is quite safe in studying the size of the higher order corrections which are described in this paper.

*Since the toponium resonance wave functions have wide distributions $\sim$ 10–20 GeV, they probe a fairly wide range of the QCD potential. For example, this is reflected in the fact that the fixed-order calculation with any single choice of scale μ cannot reproduce simultaneously both the distribution and the normalization of the differential cross section which includes all the leading logarithms. It is known that the normalization of the cross section is more sensitive to the short-distance behavior of the QCD potential.

Let us now briefly explain the construction of our potentials in momentum space and in coordinate space, respectively. More detailed descriptions including formulas are given in the appendices. The large-momentum part of the momentum-space potential $V_{\rm JKPT}(q)$ is determined as follows. First the potential has been calculated up to $\mathcal{O}(\alpha_s^3)$ in a fixed-order calculation. The result is then improved using the three-loop renormalization group equation in momentum space. At low momentum, the potential is continued smoothly to a Richardson-like potential. On the other hand, the short-distance part of the coordinate-space potential $V_{\rm SFHMN}(r)$ is calculated by taking the Fourier transform of the fixed-order potential in momentum space, and then is improved using the three-loop renormalization group equation in coordinate space. At long distance, the potential is continued smoothly to a phenomenological ansatz. Thus, it is important to note that the two potentials are *not* the Fourier transforms of each other even in the large-momentum or short-distance region. They agree only up to the next-to-next-to-leading logarithmic terms of the series expansion in a fixed $\overline{\rm MS}$ coupling. The difference begins with the non-logarithmic term in the three-loop fixed-order correction.

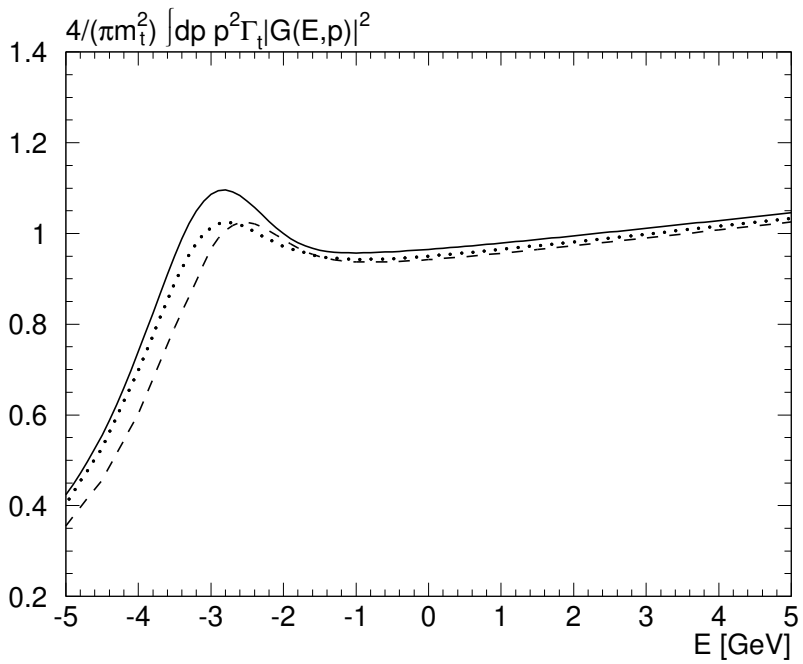

Figure 1: Comparison of the total cross sections (normalized to R) calculated from the different potentials: $V_{\rm JKPT}$ (solid), $V_{\rm SFHMN}$ (dashed), and $V_{\rm new}$ (dotted line). We set $\alpha_{\overline{\rm MS}}(M_Z^2) = 0.115$, $m_t = 175$ GeV, and $\Gamma_t = 1.427$ GeV.

In Fig. 1 we show a comparison of the total cross sections (normalized to R) calculated from $V_{\rm JKPT}$ (solid) and from $V_{\rm SFHMN}$ (dashed line), without any weak or hard-gluon corrections:

$$R = \frac{4}{\pi m_t^2} \int_0^\infty dp\, p^2 |G(E,p)|^2\, \Gamma_t. \tag{1}$$

For the physical parameters we used $\alpha_{\overline{\rm MS}}(M_Z^2) = 0.115$, $m_t = 175$ GeV, and $\Gamma_t = 1.427$ GeV.

We find that the two cross sections differ by 6.7% at the peaks and by 1.9% at $E = 5$ GeV.[†] Since the difference of the cross sections calculated from the next-to-leading order potentials is 8.2% at the peak and 2.2% at $E = 5$ GeV for the same value of $\alpha_s(M_Z^2)$ (see Figs. 5 and 6), the cross sections have come closer only slightly after the inclusion of the second-order correction to the potential. The remaining difference is much larger than what one would expect from an $\mathcal{O}(\alpha_s^3)$ correction relative to the leading order, which is not fully included in our analyses, even if we take into account the high sensitivity to the coupling, $\sigma_{\rm peak} \propto \alpha_s^2$ [1]. The purpose of this report is to understand the origin of this unexpectedly large difference.

As already mentioned, the difference of the cross sections reflects the difference of the potentials. The derivative of the potential $dV(r)/dr$ is directly related to the size of the cross section; the cross section is larger if $dV(r)/dr$ (= magnitude of the attractive force) is larger. This is because, with increasing probability that t and $\bar{t}$ stay close to each other, the wave function at the origin $|\psi(0)|^2$ increases, and so does the total cross section. Certainly, adding a constant to $V(r)$ does not affect the size of the cross section at the peak. Thus, we Fourier transformed $V_{\rm JKPT}$ numerically from momentum space to coordinate space and plot the derivatives of the potentials in Fig. 2(a). To demonstrate the difference of the attractive forces, we show the difference of the derivatives of the two potentials,

$$\Delta F(r) = \frac{dV_{\rm JKPT}(r)}{dr} - \frac{dV_{\rm SFHMN}(r)}{dr}, \tag{2}$$

(solid line) in Fig. 2(b). We confirm that $\Delta F(r) > 0$ holds in the region probed by the toponium states, $r \sim 0.03$–0.1 GeV^{-1}. One also sees that both potentials have a common slope at $r > 0.4$ GeV^{-1} because of the severe constraints from the bottomonium and charmonium data. The kink seen in the figure is due to a discontinuity of $d^2V_{\rm SFHMN}/dr^2$ located at the continuation point, $r = r_c$.

In order to compare the asymptotic behavior of the potentials more clearly, we plot in Fig. 3(a) the coordinate-space effective couplings defined by

$$\bar{\alpha}_{\rm V}(1/r) = (-C_F/r)^{-1}\, V(r) \tag{3}$$

for $V_{\rm JKPT}(r)$ and $V_{\rm SFHMN}(r)$ as solid and dashed lines, respectively. Contrary to our expectation, the difference of the couplings exceeds 3% even at very short distances, $1/r \simeq 100$ GeV.

Naturally the question arises: Why is there such a large discrepancy between the potential constructed in momentum space and that constructed in coordinate space? To answer this question, let us examine a relation connecting the effective coupling in coordinate space, defined by Eq. (3), and the effective coupling in momentum space, defined from the momentum-space potential as

$$\alpha_{\rm V}(q) = \left(-4\pi C_F/q^2\right)^{-1} V(q). \tag{4}$$

The relation is derived from the renormalization group equation of $\alpha_{\rm V}(q)$ and exact to all orders. In the asymptotic region where the couplings are small, it can be given in the form of an asymptotic series [13], which reads numerically

$$\bar{\alpha}_{\rm V}(1/r) = \alpha_{\rm V} + 1.225\,\alpha_{\rm V}^3 + 5.596\,\alpha_{\rm V}^4 + 32.202\,\alpha_{\rm V}^5 + \ldots \tag{5}$$

[†]In this paper we are not concerned with those differences of the cross sections which can be absorbed into an additive constant to the potential, or equivalently, into a redefinition of the top quark mass.

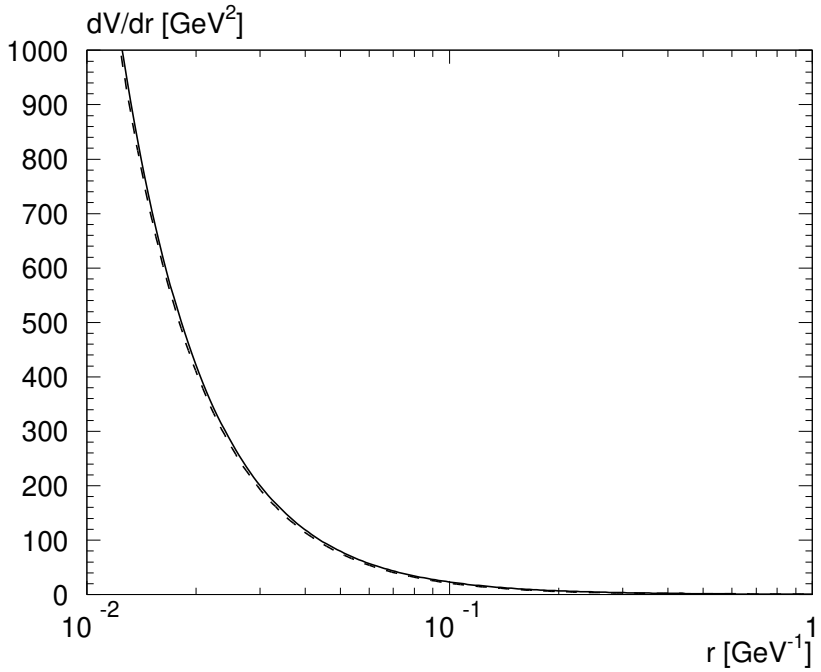

(a)

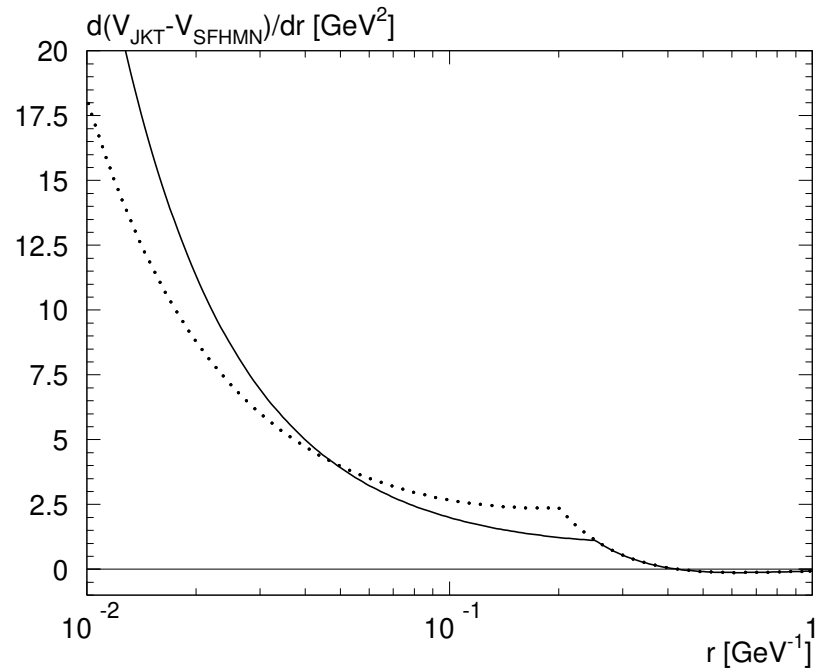

(b)

Figure 2: (a) Comparison of the derivatives of the potentials vs. r for $\alpha_{\overline{\rm MS}}(M_Z^2) = 0.115$: $dV_{\rm JKPT}/dr$ (solid line) and $dV_{\rm SFHMN}/dr$ (dashed line). (b) Difference of the derivative of the potentials vs. r. The solid line shows $\Delta F(r) = dV_{\rm JKPT}/dr - dV_{\rm SFHMN}/dr$, and the dotted line shows $\Delta F(r) = dV_{\rm JKPT}/dr - dV_{\rm new}/dr$.

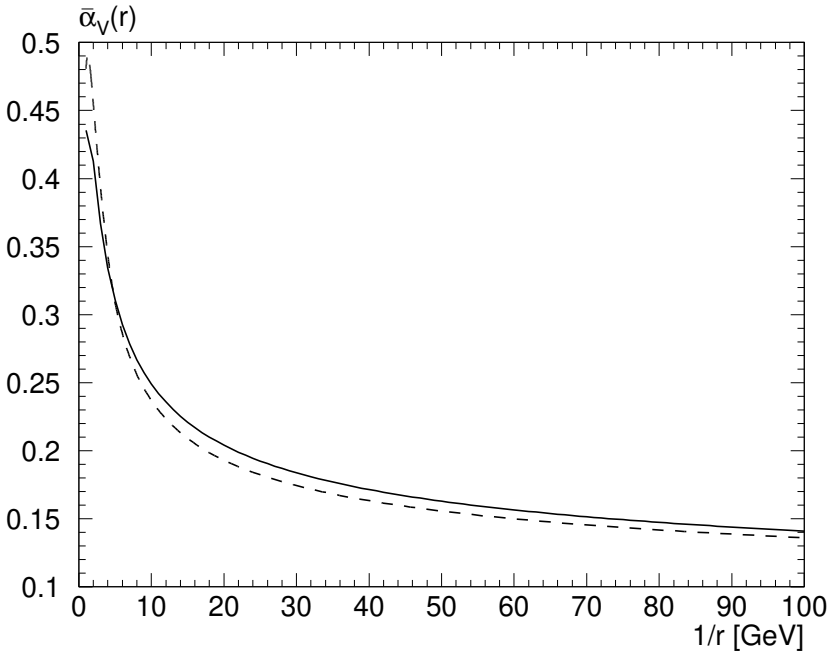

(a)

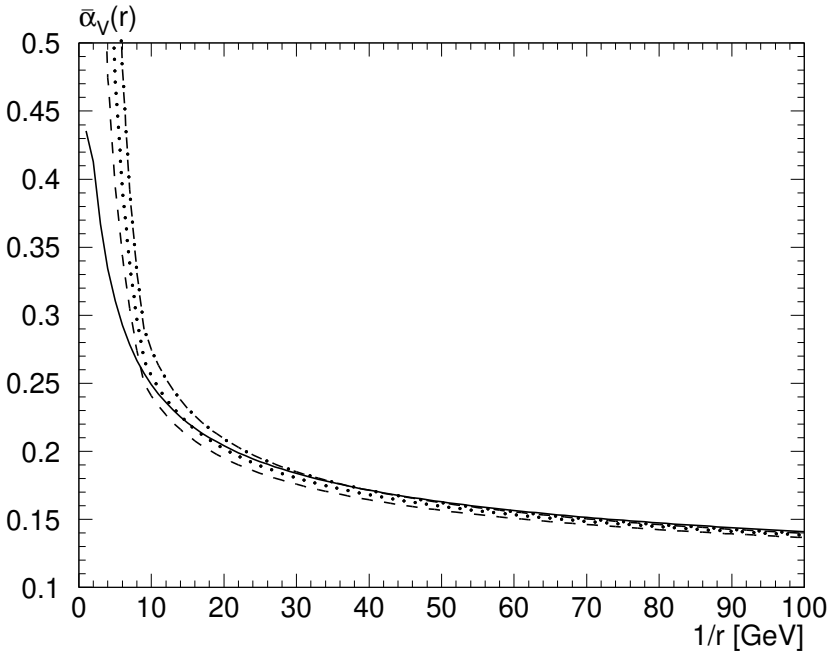

(b)

Figure 3: (a) Comparison of the coordinate-space effective charges defined from $V_{\rm JKPT}$ (solid) and from $V_{\rm SFHMN}$ (dashed line). (b) Comparison of the coordinate-space effective charges defined from the various terms of Eq. (5). See the text for the description of each curve.

for $n_f = 5$. On the right-hand-side, $\alpha_{\rm V} = \alpha_{\rm V}(q = e^{-\gamma_E}/r)$. All terms which are written explicitly are determined from the known coefficients of the β function, β_0^V, β_1^V, and β_2^V. At present, we can use the above relation consistently only at $O(\alpha_{\rm V}^3)$ because we know the effective couplings only up to the next-to-next-to-leading order corrections in perturbative QCD, i.e. we know the relation between $\alpha_{\rm V}$ and $\alpha_{\overline{\rm MS}}$ only up to $\mathcal{O}(\alpha_{\overline{\rm MS}}^3)$. Due to this limitation, essentially, the effective coupling $\bar{\alpha}_{\rm V}$ defined from $V_{\rm SFHMN}$ is the right-hand-side of the above equation truncated at the $O(\alpha_{\rm V}^3)$ term, while $\bar{\alpha}_{\rm V}$ defined from $V_{\rm JKPT}$ is the right-hand-side including all terms. Numerically, the $O(\alpha_{\rm V}^4)$ term and the $O(\alpha_{\rm V}^5)$ term contribute as +1.5% and +1.2% corrections, respectively, for $\alpha_{\rm V} \simeq 0.14$ (corresponding to $1/r = 100$ GeV). Therefore, these higher order terms indeed explain the difference of the effective couplings at small r. Fig. 3(b) shows several curves derived from the above relation:

1. The solid line is $\bar{\alpha}_{\rm V}(1/r)$ defined from $V_{\rm JKPT}$.

2. The dashed curve is $\alpha_{\rm V} + 1.225\,\alpha_{\rm V}^3$, where $\alpha_{\rm V} = \alpha_{\rm V}(q = e^{-\gamma_E}/r)$ is calculated using the perturbative prediction in momentum space. This curve is essentially the same as $\bar{\alpha}_{\rm V}(1/r)$ defined from $V_{\rm SFHMN}(r)$, since it is the next-to-next-to-leading order perturbative prediction for the coordinate-space coupling at short distances.

3. The dotted curve includes the next correction, $5.596\,\alpha_{\rm V}^4$, which is in fact even larger than the $\mathcal{O}(\alpha_{\rm V}^3)$ term below $1/r \sim 30$ GeV.

4. The dash-dotted curve includes the $\mathcal{O}(\alpha_{\rm V}^5)$ term.

We observe that the agreement of both sides of Eq. (5) becomes better as we include more terms at small r, while it becomes worse at large r on account of the asymptoticness of the series. From the purely perturbative point of view, the discrepancy between our two potentials, $V_{\rm JKPT}$ and $V_{\rm SFHMN}$, in the asymptotic region thus seems real, an indication of large higher order corrections.[‡] If the third-order correction to the potential will ever be computed in the future, the $\mathcal{O}(\alpha_V^4)$ term will be treated consistently and the difference will reduce by 1.5% at $1/r \simeq 100$ GeV.

The above 3% uncertainty of $\bar{\alpha}_{\rm V}(1/r)$ at $1/r \simeq 100$ GeV provides a certain criterion for the present theoretical uncertainty of the $t\bar{t}$ cross section. In fact, it would already limit the theoretical accuracy of $\bar{\alpha}_{\rm V}(1/r)$ at longer distances to be not better than 3%. If we combine this with a naive estimate $\sigma_{\rm peak} \propto \bar{\alpha}_{\rm V}^2$, we expect a theoretical uncertainty of the peak cross section to be $\delta\sigma_{\rm peak}/\sigma_{\rm peak} \gtrsim 6\%$. Therefore, the large discrepancy of the cross sections which we have seen turns out to be quite consistent with this estimated uncertainty.

One is tempted to include one more term of the above series (5) to define a (new) coordinate-space potential despite our ignorance of the corresponding terms in the relation between $\alpha_{\rm V}$ and $\alpha_{\overline{\rm MS}}$, since this would apparently reduce the difference between the two effective couplings. In fact we did this exercise, but (to our surprise) it did not bring the cross section closer to the one calculated from the momentum-space potential $V_{\rm JKPT}$. This cross section calculated from

[‡] If we apply the same method (the relation between $\bar{\alpha}_{\rm V}$ and $\alpha_{\rm V}$) to estimate the size of the already known $\mathcal{O}(\alpha_s^3)$ correction, we obtain $\pi^2\beta_0^2/3 = 193.4$, which turns out to be a slight under-estimate of the true correction $a_2 = 333.5$ [10] ($n_f = 5$).

the potential $V_{\rm new}(r)$, which incorporates the $\mathcal{O}(\alpha_{\rm V}^4)$ term of Eq. (5), is shown as a dotted curve in Fig. 1(b).[§]

We may understand the reason why the cross section did not approach that of $V_{\rm JKPT}$ if we look at the difference of the "forces", $\Delta F(r) = dV_{\rm JKPT}/dr - dV_{\rm new}/dr$, shown as a dotted line in Fig. 2(b): it can be seen that, upon inclusion of the $\mathcal{O}(\alpha_{\rm V}^4)$ term, the difference $\Delta F(r)$ decreased at small distances, $r < 0.05$ GeV^{-1}, as expected, whereas $\Delta F(r)$ *increased* at distances $r > 0.05\,\mathrm{GeV}^{-1}$ which is still in the range probed by the toponium states. It is due to a compensation between the decrease and increase of $\Delta F(r)$ that the normalization of the cross section scarcely changed. The increase of $\Delta F(r)$ at large distances results from the bad convergence of the asymptotic series, Eq. (5), for a large coupling, as we have already seen in Fig. 3(b). This fact indicates that we are no longer able to improve the agreement of the cross sections by including even higher order terms, as we are confronting the problem of asymptoticness of the series.

Some indications can be obtained by looking into the nature of the perturbative expansion of each potential. Within our present knowledge of the static QCD potential, the perturbative series looks more convergent for the momentum-space potential than for the coordinate-space potential. To see this, one may compare the β functions of the effective couplings (the V-scheme couplings) in both spaces [10]. Numerically, the first three terms in the perturbative expansion read

- (momentum-space coupling)

$$\mu^2 \frac{d\alpha_{\rm V}}{d\mu^2} = -0.6101\,\alpha_{\rm V}^2 - 0.2449\,\alpha_{\rm V}^3 - 1.198\,\alpha_{\rm V}^4 + \ldots \tag{6}$$

- (coordinate-space coupling)

$$\mu^2 \frac{d\bar{\alpha}_{\rm V}}{d\mu^2} = -0.6101\,\bar{\alpha}_{\rm V}^2 - 0.2449\,\bar{\alpha}_{\rm V}^3 - 1.945\,\bar{\alpha}_{\rm V}^4 + \ldots \tag{7}$$

for $n_f = 5$. The first two coefficients are universal. The third coefficient depends on the scheme (the definition) of the coupling. As the third coefficients for the V-scheme couplings are quite large, the third term of the β function is comparable to the second term already for $\alpha_V = 0.20$ and for $\bar{\alpha}_V = 0.13$, respectively.[¶] The difference of the third coefficients between momentum space and coordinate space originates from the $\pi^2\beta_0^2/3$ term in Eq. (14), which comes from the Fourier transformation. (Compare Eqs. (10) and (14).) Although the magnitude of the third coefficients is of the same order, in practice it makes a certain difference whether an apparent convergence is lost at $\alpha_V = 0.20$ or $\bar{\alpha}_V = 0.13$ because there is a large scale difference between the two values. This indicates a worse convergence in coordinate space than in momentum space.

[§]The shift of the peak position to lower energy is caused mostly by a decrease of the constant c_0 in Eq. (13) and not due to an increase of the attractive force. Since the effective coupling $\bar{\alpha}_{\rm V}(1/r)$ runs faster for $V_{\rm new}$, the perturbative potential is connected to the intermediate-distance phenomenological potential at a deeper point.

[¶]This is the reason why we evolve the $\overline{\rm MS}$ coupling instead of evolving the V-scheme couplings using their own β functions. Otherwise we would have lost the reasoning to keep the third term of the β function at a fairly large momentum/short distance. For comparison, the β function of the $\overline{\rm MS}$ coupling for the same n_f is given by

$$\mu^2 \frac{d\alpha_{\overline{\rm MS}}}{d\mu^2} = -0.6101\,\alpha_{\overline{\rm MS}}^2 - 0.2449\,\alpha_{\overline{\rm MS}}^3 - 0.09116\,\alpha_{\overline{\rm MS}}^4 + \ldots .$$

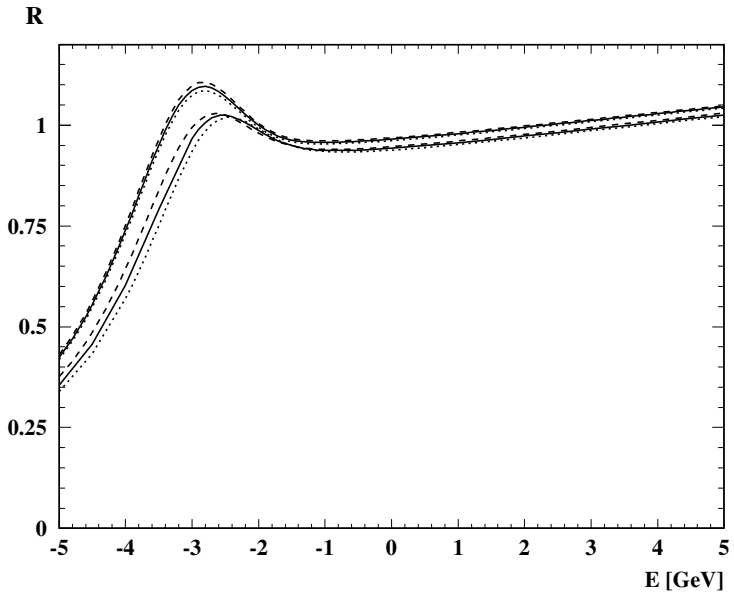

Figure 4: Comparison of the cross sections for different choices of the scale. The upper three curves are for the momentum-space approach: $\mu = q$ (solid), $\mu = \sqrt{2}q$ (dotted), and $\mu = q/\sqrt{2}$ (dashed line). The lower three curve are for the coordinate-space approach: $\mu = \mu_2 = \exp(-\gamma_E)/r$ (solid), $\mu = \sqrt{2}\mu_2$ (dotted), and $\mu = \mu_2/\sqrt{2}$ (dashed line).

If we evolve the coordinate-space coupling $\bar{\alpha}_{\rm V}$ using its own β function up to the third term, the coupling exhibits an infrared pole at $1/r = \Lambda \sim 2$ GeV, which is an order of magnitude larger than $\Lambda_{\overline{\rm MS}}$ of the $\overline{\rm MS}$ coupling. The asymptoticness of the series in Eq. (5) is closely related to the existence of this pole. In fact, one may estimate the uncertainty caused by the asymptoticness of the expansion to be $\delta\bar{\alpha}_{\rm V}(1/r) \sim \Lambda r + (\Lambda r)^2 + \ldots$ [13]. If we translate this to the uncertainty in the slope of the coordinate-space potential, we obtain $\delta F(r) \sim \Lambda^2$. This is in good agreement with the discrepancy $\Delta F(r) \sim 1$–4 GeV^2 in the region $r > 0.05$ GeV^{-1} (see Fig. 2), where the usability of the asymptotic expansion is already limited to the first two or three terms. (For $r < 0.05$ GeV^{-1}, one may reduce the difference by including more terms.)

It is interesting to examine the level of uncertainties within each of the momentum-space approach and the coordinate-space approach by itself. Fig. 4 shows how the cross section changes when we vary the scale by a factor of 2 in each approach: from $\mu = q/\sqrt{2}$ to $\mu = \sqrt{2}q$ in Eq. (28) of [10] in the momentum-space approach (upper three curves), and from $\mu = \mu_2/\sqrt{2}$ to $\mu = \sqrt{2}\mu_2$ in Eq. (44) of [10] in the coordinate-space approach (lower three curves). For the momentum-space approach, the variation of the cross section is about 2% at the peak and around 0.6% for c.m. energies above threshold. Meanwhile in the coordinate-space approach, the variation of the cross section amounts to 0.9% at the peak and 0.8% at larger c.m. energies. These results may be regarded as an internal consistency check for each approach and even as a sign for the stability of the theoretical predictions. Nevertheless one should keep in mind that the internal consistency is not the same as the accuracy of the theoretical predictions. Since

the $\mathcal{O}(\alpha_s^2)$ corrections to the potential resulted in an unexpectedly large modification of the total cross section (see Figs. 5 and 6), it would be legitimate to consider each of our results as accurate only if the same method could estimate the size of the next-to-next-to-leading order correction reasonably well and hence if the cross section became considerably less sensitive to the scale variation after including this correction. This is not the case in our problem, however. The very existence of a large constant at the next-to-next-to leading order (a_2 in [10], see also Eqs. (10) and (14)), which generates these large modifications, may indicate also large corrections at even higher orders. Furthermore, if we consider the full set of the fixed-order $\mathcal{O}(\alpha_s^2)$ corrections to the cross section near threshold [12], they are larger in size and even more scale dependent than the corrections to the potential alone. The theoretical uncertainty may therefore be larger than indicated by the study in this paper.

Still there may be some possibilities to reduce the difference between the momentum-space potential and the coordinate-space potential in the region probed by the toponium states. An obvious point to be improved is to remove the discontinuity of $V''_{\rm SFHMN}(r)$ at $r = r_c$. If we employed a smoother interpolation of the perturbative potential to the intermediate-distance potential, we would have a better agreement of the two cross sections, see Fig. 2(b). This tendency is expected due to the specific interpolation method adopted for $V_{\rm SFHMN}(r)$.[‖] However, one has to be careful with this argument. The slope of the potential in the intermediate-distance region is fixed by experimental data, which correspond to one fixed value of $\alpha_{\overline{\rm MS}}(M_Z^2)$ (= the true value in nature). We are interpolating the prediction of perturbative QCD, which obviously depends on our input value of $\alpha_{\overline{\rm MS}}(M_Z^2)$, to a phenomenological potential, which is independent of it. This means, we do expect a non-smooth transition for any value of $\alpha_{\overline{\rm MS}}(M_Z^2)$ different from the true value. Moreover, if we want to extract the value of $\alpha_{\overline{\rm MS}}(M_Z^2)$ by comparing the theoretical predictions to the experimentally measured cross section, the sensitivity to $\alpha_{\overline{\rm MS}}(M_Z^2)$ decreases if the predictions depend on the way we perform the interpolation. Ideally we would want to have an intermediate-distance potential as the prediction of QCD — necessarily non-perturbative — for a given input value of $\alpha_{\overline{\rm MS}}(M_Z^2)$.

It would be important to understand the problem of the difference in the potentials also in momentum space, at least as much as we do in coordinate space presently. We have not done this analysis so far because of the difficulty in the numerical Fourier transformation of the potential from coordinate space to momentum space.

Summary

- There is a difference between the potential constructed in momentum space and that constructed in coordinate space even at a fairly short-distance, $1/r \sim 100$ GeV. The difference can be understood within the framework of perturbative QCD. We already know that there is a large correction at $\mathcal{O}(\alpha_s^4)$ in the relation between the two potentials, although a consistent treatment is not possible until the full $\mathcal{O}(\alpha_s^4)$ corrections to the QCD potential are calculated.

[‖] $V_{\rm SFHMN}(r)$ matches the perturbative potential exactly up to a vicinity of the infrared pole. Since the rapid acceleration of the running of $\bar{\alpha}_{\rm V}(1/r)$ towards the pole tends to amplify the deviation from $V_{\rm JKPT}(r)$, if we employed an analytic regularization of the pole while keeping the potential to approximate the perturbative potential at short distances, the running of $\bar{\alpha}_{\rm V}(1/r)$ should be tamed, and hence the potential should come closer to $V_{\rm JKPT}(r)$.

- The above difference at short distances provides a criterion for our present theoretical accuracy of the $t\bar{t}$ cross section, $\delta\sigma_{\rm peak}/\sigma_{\rm peak} \gtrsim 6\%$.
- In addition, it seems that we are confronting the problem of the asymptoticness of the perturbative series in the calculation of the $t\bar{t}$ cross section, as the top quarks do not probe a region which is sufficiently deep in the potential. We may not be able to improve our theoretical precision even if the higher order corrections are calculated in perturbative QCD.
- We may, however, discuss which of the two approaches gives a more favorable result theoretically. Up to the second-order corrections, the perturbative series looks better convergent for the momentum-space potential than for the coordinate-space potential.

Acknowledgements

This work is partly supported by BMBF grant POL-239-96, by KBN grant 2P03B08414 and by the Alexander von Humboldt Foundation.

A The momentum-space potential

It seems appropriate to describe the potential $V_{\rm JKPT}$ used in the present analysis in some more detail. This potential is very similar to the potential $V_{\rm JKT}$ described in [5] and used in all later numerical studies within the momentum-space framework. It includes, however, the next-to-next-to-leading order terms from [10]. The momentum-space potential can be written as

$$V_{\rm JKPT}(\mathbf{q}) = V_0(\mathrm{q_{cut}}) \cdot (2\pi)^3\delta(\mathbf{q}) - 4\pi \mathrm{C_F}\frac{\alpha_{\rm JKPT}(\mathbf{q}^2)}{\mathbf{q}^2}. \tag{8}$$

The effective coupling $\alpha_{\rm JKPT}$ is defined to coincide with the two-loop perturbative prediction for large momenta, to be Richardson-like for small momenta, and to simply interpolate between these two shapes in some intermediate range:

$$\alpha_{\rm JKPT}(\mathbf{q}^2) = \begin{cases} \alpha_{\rm V,pert}(\mathbf{q}^2), & |\mathbf{q}| > \mathrm{q_1} = 5 \text{ GeV} \\ \alpha_{\rm Rich}(\mathbf{q}^2), & |\mathbf{q}| < \mathrm{q_2} = 2 \text{ GeV} \\ \alpha_{\rm Rich}(\mathbf{q}^2) + \frac{|\mathbf{q}|-\mathrm{q_2}}{\mathrm{q_1}-\mathrm{q_2}}\Big(\alpha_{\rm V,pert}(\mathrm{q_1^2}) - \alpha_{\rm Rich}(\mathrm{q_1^2})\Big), & \mathrm{q_2} < |\mathbf{q}| < \mathrm{q_1}. \end{cases} \tag{9}$$

The intermediate regime is only introduced to obtain a smoother transition between the small and large momentum parts, respectively.

The first difference between the updated potential and the former version is the fact that we are now able to use the full two-loop expression for the perturbative part,

$$\alpha_{\rm V,pert}(\mathbf{q}^2) = \alpha_{\overline{\rm MS}}(\mathbf{q}^2)\left(1 + a_1\frac{\alpha_{\overline{\rm MS}}(\mathbf{q}^2)}{4\pi} + a_2\Big(\frac{\alpha_{\overline{\rm MS}}(\mathbf{q}^2)}{4\pi}\Big)^2\right), \tag{10}$$

with the coefficients a_1 and a_2 given in [10]. As the b-quark threshold is neglected, $n_f = 5$ is set throughout in the evolution of the $\overline{\rm MS}$-coupling, which can now consistently be performed at three-loop accuracy.

A Richardson-like behavior for small momenta is chosen since the Richardson potential [14] is known to describe the charmonium and bottomonium spectra fairly well. A pure Richardson form, however, would lead to severe numerical problems. Hence the ansatz has to be modified slightly by introducing two "subtraction terms",

$$\alpha_{\rm Rich}(\mathbf{q}^2) = \frac{4\pi}{\beta_0(n_f=3)}\left(\frac{1}{\ln(1+\frac{\mathbf{q}^2}{\Lambda_{\rm R}^2})} - \frac{\Lambda_{\rm R}^2}{\mathbf{q}^2} + \frac{\Lambda_{\rm R}^2}{\mathbf{q}^2+{\rm q}_{\rm cut}^2}\right) \tag{11}$$

with $\Lambda_{\rm R} = 400$ MeV. The first subtraction regulates the divergent behavior for $|\mathbf{q}| \to 0$, the second subtraction is designed to reduce the modification introduced through the first to a minimum. Without the second additional term, the linear part of the position-space Richardson potential would be removed completely, whereas with it the first subtraction is cancelled for $\mathbf{q}^2 \gg {\rm q}_{\rm cut}^2$, and thus a big part of the confining potential is kept. It thus seems desirable to choose the parameter $\rm q_{cut}$ small, but evidently it cannot be put to zero to really recover the pure Richardson potential. However, the linear part of the potential plays practically no role for the $t\bar{t}$-system as will be demonstrated below. The exact value of $\rm q_{cut}$ is therefore relatively unimportant and the adopted value $\rm q_{cut} = 50$ MeV results in both numerical efficiency and speed of the program and a fairly good accuracy of the predictions.

The constant $V_0(\rm q_{cut})$ in Eq. (8) is to some extent an arbitrary parameter. Different choices of $V_0(\rm q_{cut})$ reflect the ambiguity in the definition of the pole masses for confined quarks. For $V_{\rm JKPT}(\mathbf{q})$ the choice

$$V_0(\rm q_{cut}) = \frac{4\pi {\rm C_F}}{\beta_0({\rm n_f}=3)}\frac{\Lambda_{\rm R}^2}{\rm q_{cut}} \tag{12}$$

is used. It leads to a Richardson-like potential that depends only weakly on the parameter $\rm q_{cut}$ and coincides with the true Richardson potential in position space in the limit $\rm q_{cut} \to 0$. With this potential one obtains for the pole mass of the b quark $m_b = 4.84$ GeV. The choice of V_0 is the second difference to the potential used in earlier works, where the constant V_0 was fixed by the condition $V_{JKT}(r = 1\ {\rm GeV}^{-1}) = -1/4$ GeV leading to $m_b = 4.7$ GeV.

Fig. 5 shows a comparison of the total cross section for $t\bar{t}$-production near threshold as a function of energy using the "old" potential, i.e. the one as described but using the one-loop formula for $\alpha_{\rm V,pert}$ (and correspondingly the two-loop evolution for the $\overline{\rm MS}$-coupling) and fixing V_0 through $V(r = 1\ {\rm GeV}^{-1}) = -1/4$ GeV (dash-dotted line), and the "new" potential (solid line). There are two changes: first, the inclusion of the two-loop correction to the perturbative potential increases the strength of the attractive interaction between t and $\bar{t}$, and thus leads to an increase in the cross section. This is nicely demonstrated by the dashed curve, which corresponds to the inclusion of the two-loop potential, but the old choice of V_0. Second, the modified choice for V_0 leads to a small shift of about 300 MeV in the energy scale, which is just the difference between the two V_0. The dotted curve has been included to once again demonstrate that the $t\bar{t}$ system is quite insensitve to the long-range part of the potential: this curve corresponds to the choice $\rm q_{cut} = \infty$, i.e. to completely removing the linear part from the potential and setting $V_0 = 0$.

B The coordinate-space potential

The short-distance part of the coordinate-space potential is given by the next-to-next-to-leading order static QCD potential in position space [10], whereas its form in the intermediate- and

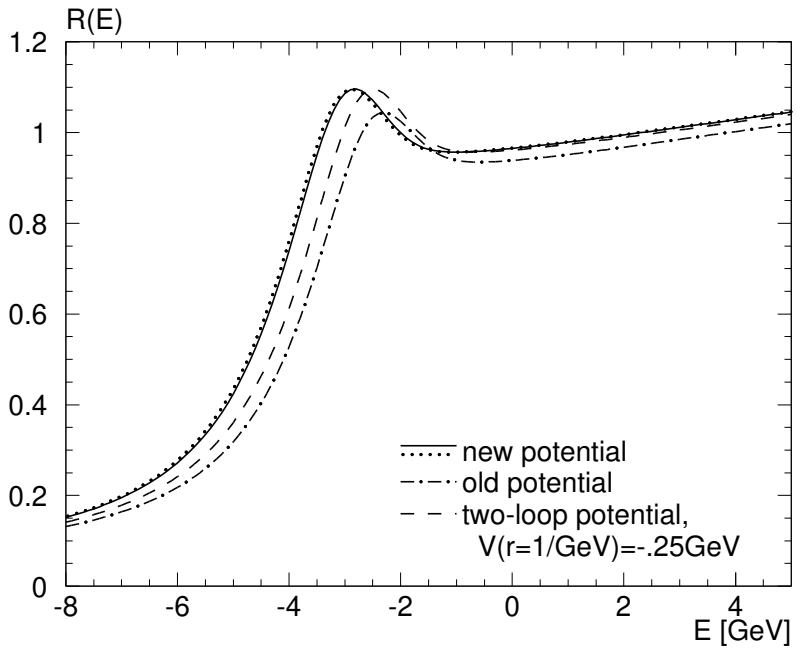

Figure 5: Comparison of the total cross section (normalized to R) for $t\bar{t}$-production as a function of $E = \sqrt{s} - 2m_t$ for $m_t = 175$ GeV, $\alpha_{\overline{\rm MS}} = 0.115$, and $\Gamma_t = 1.427$ GeV, using the different potentials described in the text. The dash-dotted line corresponds to the model of older analyses, the dashed line to the inclusion of the two-loop correction to the perturbative part. The solid line shows the prediction of the new model, which differs from the dashed line only by a different definition of the energy. The dotted line corresponds to the new potential with the linear part in position space removed.

long-distance region is determined phenomenologically. We thus have

$$V_{\rm SFHMN}(r) = \begin{cases} V_{\rm pert}(r) & \text{at} \quad r < r_c\,, \\ c_0 + c_1 \log(r/r_0) \exp(-r/r_1) + ar & \text{at} \quad r > r_c\,. \end{cases} \tag{13}$$

Here,

$$V_{\rm pert}(r) = -C_F \frac{\alpha_{\overline{\rm MS}}(\mu_2^2)}{r} \left[1 + a_1 \frac{\alpha_{\overline{\rm MS}}(\mu_2^2)}{4\pi} + \Big(a_2 + \frac{\pi^2 \beta_0^2}{3}\Big) \Big(\frac{\alpha_{\overline{\rm MS}}(\mu_2^2)}{4\pi}\Big)^2 \right] \tag{14}$$

represents the coordinate-space potential in the second scheme, $\mu_2 = \exp(-\gamma_E)/r$. The coefficients a_1 and a_2 are the same as in the momentum-space potential, and $\beta_0 = (11 C_A - 4 T_F n_f)/3$. See Ref. [10] for details.**

The values of the phenomenological parameters r_0, r_1, a and c_1 are taken from Ref. [3] and

**We evolve the $\overline{\rm MS}$-coupling $\alpha_{\overline{\rm MS}}(\mu)$ by solving the three-loop renormalization group equation *numerically* for a given initial value at $\mu = M_Z$, whereas an approximate solution to the renormalization group equation is used in [10].

are tuned to reproduce bottomonium and charmonium data well:

$$\begin{array}{lcll} r_0 & = & 0.2350 & \mathrm{GeV}^{-1} \\ r_1 & = & 3.745 & \mathrm{GeV}^{-1} \\ a & = & 0.3565 & \mathrm{GeV}^{-2} \\ c_1 & = & 0.8789 & \mathrm{GeV} \end{array} \tag{15}$$

We fix c_0 and r_c by requiring that both the potential $V_{\rm SFHMN}(r)$ and its first derivative are continuous at $r = r_c$. For example, $r_c = 0.2526$ GeV^{-1} and $c_0 = -1.972$ GeV for $\alpha_{\overline{\rm MS}}(M_Z^2) = 0.115$.

This potential is an improved version of the potential proposed in [3] by including the next-to-next-to leading order terms to the short-distance QCD potential. We compare the cross sections calculated from the present version and from the old version in Fig. 6 for $\alpha_{\overline{\rm MS}}(M_Z^2) = 0.115$.

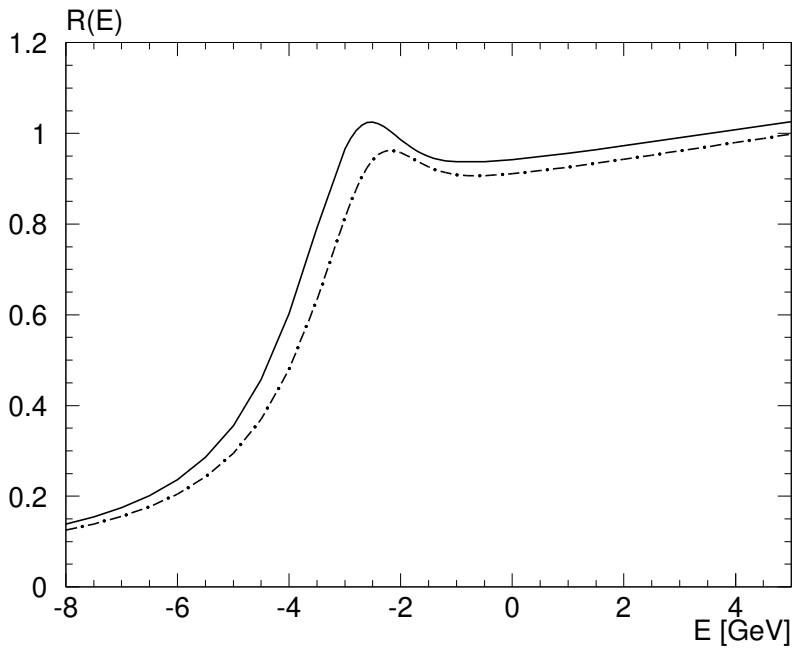

Figure 6: Comparison of the total cross section (normalized to R) as a function of $E = \sqrt{s} - 2m_t$ for $m_t = 175$ GeV, $\alpha_{\overline{\rm MS}} = 0.115$ and and $\Gamma_t = 1.427$ GeV using the old and the present versions of the coordinate-space potential $V_{\rm SFHMN}$. The dash-dotted line corresponds to the potential described in [3]. The solid line shows the prediction of the present potential, Eq. (13).

References

[1] M.J. Strassler and M.E. Peskin, *Phys. Rev.* **D43** (1991) 1500.

[2] V.S. Fadin and V.A. Khoze, *JETP Lett.* **46** (1987) 525; *Sov. J. Nucl. Phys.* **48** (1988) 309.

[3] Y. Sumino, K. Fujii, K. Hagiwara, H. Murayama and C.-K. Ng, *Phys. Rev.* **D47** (1993) 56.

[4] M. Jeżabek, J.H. Kühn and T. Teubner, *Z. Phys.* **C56** (1992) 653.

[5] M. Jeżabek and T. Teubner, *Z. Phys.* **C59** (1993) 669.

[6] M. Peter and Y. Sumino, University of Karlsruhe Report No. TTP97-27, hep-ph/9708223, to appear in *Phys. Rev.* **D**.

[7] A.H. Hoang, *Phys. Rev.* **D56** (1997) 5851.

[8] A.H. Hoang, P. Labelle and S.M. Zebarjad, *Phys. Rev. Lett.* **79** (1997) 3387.

[9] G. Adkins, R.N. Fall and P.M. Mitrikov, *Phys. Rev. Lett.* **79** (1997) 3383.

[10] M. Peter, *Phys. Rev. Lett.* **78** (1997) 602; *Nucl. Phys.* **B501** (1997) 471.

[11] A. Czarnecki and K. Melnikov, University of Karlsruhe Report No. TTP97-54, hep-ph/9712222, and references therein.

[12] A. Hoang and T. Teubner, University of California, San Diego Report No. UCSD/PTH 98-01, DESY 98-008, hep-ph/9801397.

[13] M. Jeżabek, M. Peter and Y. Sumino, in preparation.

[14] J.L. Richardson, *Phys. Lett.* **B82** (1979) 272.